Intracranial Migration of Silicone Delaying Life Saving Surgical Management: A Mimicker of Hemorrhage

Dani Sarohia[1*], Ramin Javan[1], Salim Aziz[2]

1. Department of Radiology, George Washington University Hospital, Washington D.C., USA

2. Department of Cardiothoracic Surgery, George Washington University Hospital, Washington D.C., USA

* **Correspondence:** Dani Sarohia, George Washington University Hospital, Department of Radiology, 900 23rd Street NW, Suite G2092, Washington DC 20037, USA
(✉ *Dani_sarohia@ gwu.email.edu*)

ABSTRACT

We present a case in which intraocular silicone injection for complex retinal detachment resulted in migration and distribution of silicone along the intracranial visual pathway, and ultimately throughout the ventricular system. Misinterpretation of this material as intracranial hemorrhage on outside computed tomography imaging delayed emergent repair of a Type A aortic dissection until the diagnosis was made on repeat imaging. A discussion of this case and salient computed tomography and magnetic resonance imaging characteristics of silicone is provided.

CASE REPORT

CASE REPORT

PRESENTATION WITH CLINCAL AND EXAM FINDINGS

A 51-year-old female with history of Marfan syndrome, multiple retinal detachments resulting in bilateral blindness, and history of prior Type B aortic dissection, presented to an outside hospital with acute onset chest and back pain, and sluggish speech. She also complained of left sided weakness with 3/5 strength in the left upper and lower extremities and intact reflexes. Ocular exam revealed bilateral blindness. Initial imaging studies included computed tomography angiography (CTA) of the chest, abdomen, and pelvis and non-contrast computed tomography (CT) of the head.

INITIAL IMAGING FEATURES

CT of the chest demonstrated a Debakey Type I/Stanford Type A aortic dissection extending from the aortic root superiorly to involve the common and internal carotid arteries (Figure 1). Non-contrast CT head showed multiple hyperdense foci most strikingly filling the fourth ventricle, which in the acute setting was interpreted as acute intraventricular and subarachnoid hemorrhage (Figure 2). She was subsequently transferred to our institution where several imaging studies were performed in close succession including magnetic resonance imaging (MRI) of the brain, and CTA of the head and neck. MRI brain performed overnight during the weekend demonstrated partially T1 hyperintense material in the suprasellar cistern as well as the third and fourth ventricles. Signal dropout in these regions was seen on gradient echo and susceptibility weighted imaging (Figure 3). In concert with the outside CT head interpretation, this was preliminarily deemed compatible with blood products. Magnetic resonance angiography (MRA) of the head and neck was also performed showing known aortic dissection extending into the common and internal carotid arteries. The study however was non-diagnostic for evaluation of the intracranial vasculature due to motion artifact.

REPEAT IMAGING AND EVALUATION

In accordance with the above conclusions, surgical repair of the dissection was delayed and the patient was stabilized in the intensive care unit (ICU). CT angiography of the head and neck was obtained within 4 days of the initial outside CT to evaluate for potential causes of intracranial hemorrhage, specifically aneurysms, as MR angiography performed earlier was non-diagnostic. Hyperdense material was again noted predominantly in the third ventricle and fourth ventricles, as well along the left optic nerve sheath, the optic chiasm, and a trace amount in the frontal horn of the right lateral ventricle (Figure 4).

Several critical additional observations were made during interpretation of this exam. First, the hyperdense material originally thought to represent hemorrhage appeared identical to the hyperdense material noted on the original outside head CT performed four days earlier (Figures 2, 4). Such stability over several days of imaging is extremely atypical for evolving hemorrhagic products. Second, we observed that the density and intensity of the presumed blood products in the ventricular system and the optic chiasm were identical to the density and intensity of the intraocular silicone in the left globe and optic nerve on both CT and MR (Figures 2, 3, 4). Third, on re-examination, MR brain notably demonstrated chemical shift artifact. Fourth, the hyperdense/hyperintense material in the right lateral ventricle assumed a non-dependent position in the frontal horn, atypical for dense hemorrhagic products, which gravity dictates layers dependently in the occipital horns (Figures 2C, 3G, H). Lastly, it has been shown that blood products may exhibit restricted diffusion [1, 2]. In our case the lack of restricted diffusion in the areas corresponding with hyperdense foci on CT images again points one toward the appropriate conclusion that the material is in fact silicone, not blood.

TREATMENT

Shortly after this, the patient was taken to the operating room (OR) as intracranial bleed had been excluded. She underwent replacement of the ascending aorta with a graft and repair of the aortic valve. Following surgery she was returned to the ICU in stable condition.

DISCUSSION

Etiology & Demographics:

Intraocular silicone oil injection has been used for many years in the repair of retinal detachment. Detachment occurs when subretinal fluid collects in a potential space between the neurosensory retina and the retinal pigment epithelium. Three types have been described, rhegmatogenous, tractional, and exudative. Rhegmatogenous is the most common, occurring when a tear in the peripheral retina results in separation of the retinal layers with vitreous fluid accumulation between them [3]. This causes progressive visual loss. The incidence of retinal detachment is 1:10,000. Initial attempts at repair of rhegmatogenous detachment usually involve scleral buckling, successful in 80-90% of cases. In more complex cases intraocular tamponade with injection of gas and/or silicone oil is performed. Several known side effects include cataract

formation, silicone oil keratopathy, emulsification of oil with glaucoma, intraconjunctival oil inclusion cysts, subretinal oil, reproliferation of membranes beneath the oil interface, and optic atrophy [4]. Currently there is no consensus on the practice and timing of silicone removal, which is generally decided on a case-by-case basis.

The phenomenon of intracranial migration of silicone used for treatment of complex retinal detachment has been described in only a handful of radiology case reports. Of the reported cases, this is observed in patients ranging in age from 15 to 80, in slightly more males than females. Most patients suffered retinal detachment as a result of HIV associated CMV retinitis, or diabetic retinopathy. Interestingly, more often than not, these patients were observed to have elevated intraocular pressure. While patients were generally asymptomatic, reported symptoms include seizures, headaches, dizziness, and nausea [5-10]. The current literature suggests that heavy tamponade is becoming increasingly common as newer and safer silicone-containing agents such as Oxane HD and Densiron 68 have been developed with minimal reported side effects [11]. Our case serves to demonstrate the critical importance of differentiating this entity from intracranial hemorrhage for effective patient management, especially in the acute setting.

Pathophysiology & Anatomy:

The mechanism by which intraocular silicone enters the subarachnoid space and the ventricular system is uncertain as there is no anatomic connection between the vitreous and the intracranial subarachnoid space. Reviewing the anatomy reveals that the axons of the retinal ganglion cells converge from all over the retina to become the intraocular segment of the optic nerve, or the optic disc. The optic nerve exits the globe through the lamina cribrosa, an opening of the sclera composed of a network of collagen fibers forming small canals, which are traversed by optic nerve axons. From this point forth the optic nerve is closely invested by, from inner to outer, pia, cerebrospinal fluid (CSF) and arachnoid, and dura mater. This transition is important in that the peri-neural subarachnoid space surrounding the intraorbital segment of the optic nerve is continuous with the intracranial subarachnoid space. The nerve then traverses the orbit, passes through the orbital canal within the lesser wing of the sphenoid, and exits the annulus of Zinn in the intracanalicular segment, to become the intracranial segment within the suprasellar cistern [12, 13].

A literature review revealed several possible mechanisms enumerated in Table 4. In all theories, different mechanisms, including increased intraocular pressure, congenital abnormalities in the optic nerve, and cavernous degeneration of the optic nerve, lead to a common pathway. That is, silicone migration through the pial layer investing the optic nerve to the subarachnoid space of the optic nerve, in continuity with the intracranial subarachnoid space. The intracranial subarachnoid space is connected to the ventricular system via the foramen of Luschka and Magendie. To our knowledge, intracranial migration of intravitreal silicone has not been reported in a patient with Marfan syndrome, especially in a situation where initial misdiagnosis had led to delay in emergent life-saving surgical management.

Marfan syndrome is caused by a defect in the fibrillin gene on chromosome 15. Fibrillin is a key component in extracellular microfibrills found throughout the body. Importantly, fibrillin is a key structural component in the ciliary body, one of the reasons ectopia lentis is commonly found in Marfan patients. In addition fibrillin has been mapped to the lamina cribrosa, the sclera, the choroid, and Bruch's membrane (innermost layer of the choroid). Given this anatomic distribution, structural abnormalities of the orbit, specifically the lamina cribrosa seen in Marfan syndrome may facilitate migration of silicone directly through the lamina cribrosa, across the pia and into the peri-neural subarachnoid space. It is also important to note that Marfan syndrome predisposes patients to aortic aneurysms and dissection, as fibrillin is present in the wall of the aorta. Some of the potential imaging findings in patients with Marfan syndrome are discussed in Table 5 [14, 15].

Clinical & Imaging Findings:

The main challenge in cases such as ours is distinguishing silicone from subarachnoid hemorrhage. The causes of subarachnoid hemorrhage are divided into two categories, traumatic and spontaneous. Trauma is the most common cause of subarachnoid hemorrhage. Spontaneous subarachnoid hemorrhage is most commonly caused by aneurysm rupture, accounting for 85% of cases. Approximately 10% are caused by are perimesencephalic hemorrhage, which are thought to be mostly venous in origin. The remaining 5% of cases have relatively rare causes such as vascular malformations and venous infarction. Non-contrast CT head shows hyperdensity in the basilar cisterns and sylvian fissures. In the acute phase the FLAIR sequence similarly shows hyperintense signal in the basilar cisterns and sylvian fissures [16].

Regardless of its location in the eye, the optic pathway, or the ventricular system, silicone has unique imaging characteristics, which may be used to distinguish it from hemorrhage (Table 3). On CT silicone appears hyperdense, in fact denser than typical hemorrhagic products. The Hounsfield unit (HU) measurement of silicone has been reported as high as 132 in an older study in which CT was performed on a silicone oil/water phantom. In more recent studies intraocular and intraventricular silicone has been reported to have densities of 115, 106, and 90 Hounsfield units [17]. In contrast, the density of blood is generally 30-60 HU, and almost always less than 90 HU. In our case, the density of intraventricular silicone measured approximately 100 HU [5, 18].

Blood has varying intensities on MR T1 weighted images (T1WI) and T2 weighted images (T2WI) depending on age, with methemoglobin in subacute blood appearing T1 hyperintense. The CT and MR imaging characteristics of intraparenchymal hemorrhage are discussed in table 4 below. It should be noted however that the evolution of subarachnoid and intraventricular hemorrhage is somewhat different than this primarily due to the face that blood products in these spaces mix with cerebrospinal fluid [19, 20]. Silicone in the ventricles appears hyperintense in comparison with CSF on T1 weighted images, and of variable intensity on T2 images depending on the viscosity of the silicone, field strength, and sequence parameters. Both blood and silicone demonstrate increased

susceptibility artifact. However, two distinguishing factors may be utilized to distinguish them. First, silicone is less dense (volumetric mass density) than CSF, and thus will appear in a non-dependent location within the ventricular system as it did in our case. Also, and perhaps more importantly, at the interface between silicone and brain parenchymal tissue there is a prominent chemical shift artifact seen on T2/fluid attenuated inversion recovery (FLAIR) and T1 imaging. This is secondary to differences in the resonant frequencies, i.e. frequency direction of silicone and water, and is manifested as a bright line on one side and a dark line on the other end of the interface between silicone and water [5-9]. A third distinguishing factor is seen on diffusion-weighted imaging. Specific stages of intracranial hematoma show restricted diffusion. One study showed more specifically that the core of hyperacute and late subacute hematomas show restricted diffusion [1, 2]. Notably, the regions of intraocular and intraventricular T1 hyperintensity on our patient's MR brain did not demonstrate restricted diffusion. Because some stages of hematoma may also not show restricted diffusion, this characteristic may be used only in conjunction with other imaging characteristics in ruling out intracranial hemorrhage.

The diagnosis of intraventricular silicone may be made with reasonable confidence given the multitude of specific imaging characteristics discussed above. However if 100% certainty is sought, silicone specific imaging strategies in vivo and vitro may be employed. Mathews et al performed proton MR spectroscopy on silicone in vitro, finding the silicone peak to be .33 ppm [17]. Tatewaki et al report the first case in which intraventricular silicone in a 66-year-old woman presenting with sudden onset lower extremity weakness was definitively identified with proton MR spectroscopy, finding an identical peak at .33 ppm [8].

Treatment & Prognosis:

In the majority of cases intracranial silicone is found incidentally. In one reported case a patient with intraventricular silicone was treated with a ventriculoperitoneal shunt, having suffered from headaches [10]. In the remainder of the reported cases, this entity was identified to the exclusion of other etiologies such as hemorrhage and neoplasm, but not treated, as patients were generally asymptomatic. Prognosis is unknown.

Differential Diagnoses:

Apart from subarachnoid hemorrhage, the differential diagnosis for intraventricular silicone includes several entities that may be mistaken for intracranial hemorrhage, termed pseudo-subarachnoid hemorrhage [21].

Spontaneous intracranial hypotension

Spontaneous intracranial hypotension (SIH), a type of pseudo-subarachnoid hemorrhage, presents with orthostatic headache, low CSF pressure, and distinct imaging characteristics. SIH may be mistaken for subarachnoid hemorrhage on CT, usually the first imaging procedure performed in an emergency situation. Increased attenuation is seen in the basilar cisterns and the sylvian fissures. This appearance has been postulated to occur as a result of brain sagging, a characteristic feature of SIH seen on MR. The

sagging causes compression of the subarachnoid spaces causing displacement of hypodense CSF. The denser meningeal layers and blood vessels in this region, including the middle meningeal artery and the basal veins of Rosenthal, then fill a larger percentage of the subarachnoid space mimicking subarachnoid hemorrhage. Clinical symptoms occurring with SIH and SAH, such as thunderclap headache, nausea, vomiting, neck pain, may be similar and thus not helpful in distinguishing the two entities. Magnetic resonance imaging characteristics seen in SIH, namely diffuse pachymeningeal enhancement and brain sagging may be of the most utility arriving at the diagnosis [21].

Leptomeningitis

Leptomeningitis is another cited cause of pseudo-subarachnoid hemorrhage. In many instances patients with leptomeningeal infection may have a normal non-contrast head CT. However it has been postulated that purulent exudate within the CSF space may mimic the appearance of subarachnoid hemorrhage. On post contrast CT head enhancement may be observed due to cerebritis and breakdown of the blood brain barrier. MR brain in leptomeningitis also shows hyperintense T1 signal in the basilar cisterns, and post-contrast leptomeningeal enhancement. Additionally the clinical history of infectious symptoms may be helpful in distinguishing these two entities [22].

Hypoxic ischemic encephalopathy

On non-contrast head CT exams of patients with hypoxic encephalopathy after resuscitation from cardiopulmonary arrest, hyperdensity in the basilar cisterns and sulci has been observed. This occurs specifically in patients with marked cerebral edema. Several authors have suggested the mechanism for this. The low attenuation of the edematous brain parenchyma, and distension of the superficial cortical veins secondary to compression of the dural sinuses by brain edema causes a relatively dense appearance within the subarachnoid space [23]. In the emergency situation, CT is again usually the first imaging test, however MR findings differentiate this entity from the above differentials. Gray matter structures including the basal ganglia, thalami, cortex, cerebellum, and hippocampi are affected showing restricted diffusion within the first few hours. Between 24 hours and two weeks these structures demonstrate T2 hyperintensity and swelling. After two weeks T1 hyperintensity is seen due to cortical laminar necrosis [24].

Intracranial silicone

In our case, of course, the intraventricular and subarachnoid hyperdense material mistaken for blood was in fact intracranial silicone, originating from the patient's left globe.

Conclusion:

Silicone oil has been and will be used not infrequently as a method of treatment of complex retinal detachment especially due to the development of newer safer heavy tamponades, such as Oxane HD and Densiron 68 [11]. Radiologists should be familiar with the basic imaging characteristics of silicone oil and be able to distinguish it from intracranial hemorrhage. In our case, the patient happened to also require emergent

surgical treatment of a potentially fatal condition, making the recognition of intracranial silicone critical in her management.

TEACHING POINT

Intraocular injected silicone may migrate from the vitreous into the subarachnoid space of the optic sheath surrounding the intraorbital segment of the optic nerve to eventually settle in the intracranial subarachnoid spaces and the intraventricular system, mimicking intracranial hemorrhage. The unique characteristics of silicone including high density (HU > 90), non-dependent location within the ventricles, identical appearance on follow-up imaging, as well as presence of chemical shift artifact evident on MR imaging, can be utilized in differentiating silicone from blood in the acute setting.

REFERENCES

1. Atlas SW, DuBois P, Singer MB, Lu D. Diffusion measurements in intracranial hematomas: implications for MR imaging of acute stroke. AJNR Am J Neuroradiol, 2000. 21(7): p. 1190-4. PMID: 10954267

2. Silvera S, Oppenheim C, Touze E, Ducreux D, Page P, Domigo V, et al. Spontaneous intracerebral hematoma on diffusion-weighted images: influence of T2-shine-through and T2-blackout effects. AJNR Am J Neuroradiol, 2005. 26(2): p. 236-41. PMID: 15709118

3. La Heij EC Hendrikse F. Retinal detachments and retinal surgery. Ned Tijdschr Geneeskd, 1999. 143(15): p. 781-5. PMID: 10347640

4. Eller AW, Friberg TR, Mah F. Migration of silicone oil into the brain: a complication of intraocular silicone oil for retinal tamponade. Am J Ophthalmol, 2000. 129(5): p. 685-8. PMID: 10844074

5. Chen JX NA, Aygun N, Gujar SK, Gandhi D. Intravitreal silicone oil migration into the subarachnoid space and ventricles: A case report and review of literature. European Journal of Radiology Extra 2011. 78, e81-e83. Not referenced.

6. Kim H, Hong HS, Park J, Lee AL. Intracranial Migration of Intravitreal Silicone Oil: A Case Report. Clin Neuroradiol, 2015. PMID: 25722020

7. Murray JG, Gean AD, Barr RM. Intraocular silicone oil for retinal detachment in AIDS: CT and MR appearances. Clin Radiol, 1996. 51(6): p. 415-7. PMID: 8654006

8. Tatewaki Y, Kurihara N, Sato A, Suzuki I, Ezura M, Takahashi S. Silicone oil migrating from intraocular tamponade into the ventricles: case report with magnetic resonance image findings. J Comput Assist Tomogr, 2011. 35(1): p. 43-5. PMID: 21245688

9. Williams RL, Beatty RL, Kanal E, Weissman JL. MR imaging of intraventricular silicone: case report. Radiology, 1999. 212(1): p. 151-4. PMID: 10405734

10. Hruby PM, Poley PR, Terp PA, Thorell WE, Margalit E. Headaches secondary to intraventricular silicone oil successfully managed with ventriculoperitoneal shunt. Retin Cases Brief Rep, 2013. 7(3): p. 288-90. PMID: 25391126

11. Heimann H, Stappler T, Wong D. Heavy tamponade 1: a review of indications, use, and complications. Eye (Lond), 2008. 22(10): p. 1342-59. PMID: 18344952

12. Elkington AR, Inman CB, Steart PV, Weller RO. The structure of the lamina cribrosa of the human eye: an immunocytochemical and electron microscopical study. Eye (Lond), 1990. 4 (Pt 1): p. 42-57. PMID: 2182351

13. Prasad S, Galetta SL. Anatomy and physiology of the afferent visual system. Handb Clin Neurol, 2011. 102: p. 3-19. PMID: 21601061

14. Ha HI, Seo JB, Lee SH, Kang JW, Goo HW, Lim TH, et al. Imaging of Marfan syndrome: multisystemic manifestations. Radiographics, 2007. 27(4): p. 989-1004. PMID: 17620463

15. Nemet AY, Assia EI, Apple DJ, Barequet IS. Current concepts of ocular manifestations in Marfan syndrome. Surv Ophthalmol, 2006. 51(6): p. 561-75. PMID: 17134646

16. van Gijn J Rinkel GJ. Subarachnoid haemorrhage: diagnosis, causes and management. Brain, 2001. 124(Pt 2): p. 249-78. PMID: 11157554

17. Mathews VP, Elster AD, Barker PB, Buff BL, Haller JA, Greven CM. Intraocular silicone oil: in vitro and in vivo MR and CT characteristics. AJNR Am J Neuroradiol, 1994. 15(2): p. 343-7. PMID: 8192083

18. Chang CC, Chang HS, Toh CH. Intraventricular silicone oil. J Neurosurg, 2013. 118(5): p. 1127-9. PMID: 23350782

19. Parizel PM, Makkat S, Van Miert E, Van Goethem JW, van den Hauwe L, De Schepper AM. Intracranial hemorrhage: principles of CT and MRI interpretation. Eur Radiol, 2001.

11(9): p. 1770-83. PMID: 11511901

20. Whang JS, Kolber M, Powell DK, Libfeld E. Diffusion-weighted signal patterns of intracranial haemorrhage. Clin Radiol, 2015. 70(8): p. 909-16. PMID: 26050534

21. Ferrante E, Regna-Gladin C, Arpino I, Rubino F, Porrinis L, Ferrante MM, et al. Pseudo-subarachnoid hemorrhage: a potential imaging pitfall associated with spontaneous intracranial hypotension. Clin Neurol Neurosurg, 2013. 115(11): p. 2324-8. PMID: 24075686

22. Mendelsohn DB, Moss ML, Chason DP, Muphree S, Casey S, Acute purulent leptomeningitis mimicking

subarachnoid hemorrhage on CT. J Comput Assist Tomogr, 1994. 18(1): p. 126-8. PMID: 8282861

23. Yuzawa H, Higano S, Mugikura S, Umetsu A, Murata T, Nakagawa A, et al. Pseudo-subarachnoid hemorrhage found in patients with postresuscitation encephalopathy: characteristics of CT findings and clinical importance. AJNR Am J Neuroradiol, 2008. 29(8): p. 1544-9. PMID: 18556358

24. Huang BY Castillo M. Hypoxic-ischemic brain injury: imaging findings from birth to adulthood. Radiographics, 2008. 28(2): p. 417-39; quiz 617. PMID: 18349449

25. Fangtian D, Rongping D, Lin Z, Weihong Y. Migration of intraocular silicone into the cerebral ventricles. Am J Ophthalmol, 2005. 140(1): p. 156-8. PMID: 16038670

26. Kuhn F, Kover F, Szabo I, Mester V. Intracranial migration of silicone oil from an eye with optic pit. Graefes Arch Clin Exp Ophthalmol, 2006. 244(10): p. 1360-2. PMID: 16523301

27. Papp A, Toth J, Kerenyi T, Jackel M, Suveges I. Silicone oil in the subarachnoidal space--a possible route to the brain? Pathol Res Pract, 2004. 200(3): p. 247-52. PMID: 15200277

28. Shields CL, Eagle RC Jr. Pseudo-Schnabel's cavernous degeneration of the optic nerve secondary to intraocular silicone oil. Arch Ophthalmol, 1989. 107(5): p. 714-7. PMID: 2719581
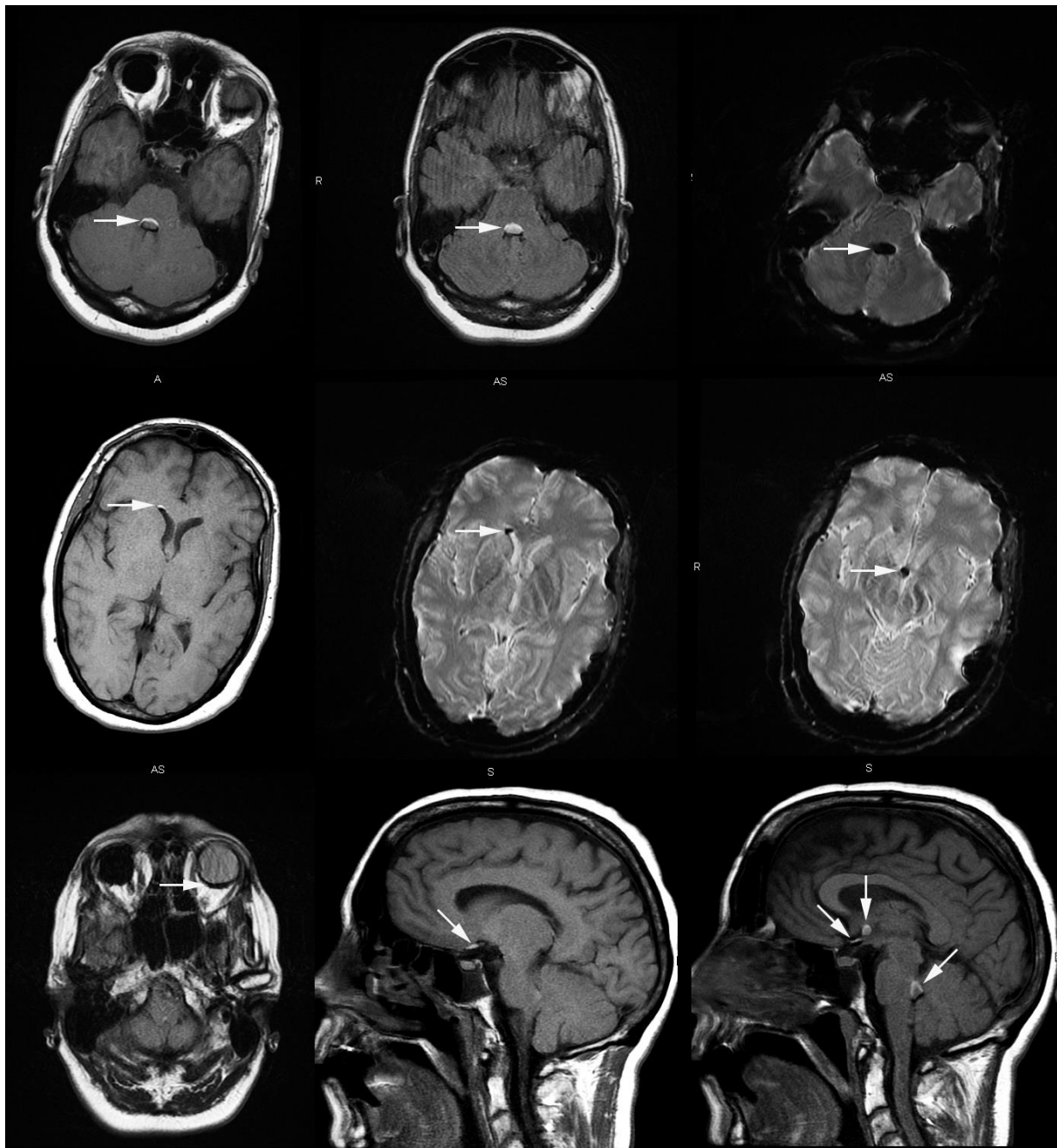
FIGURES
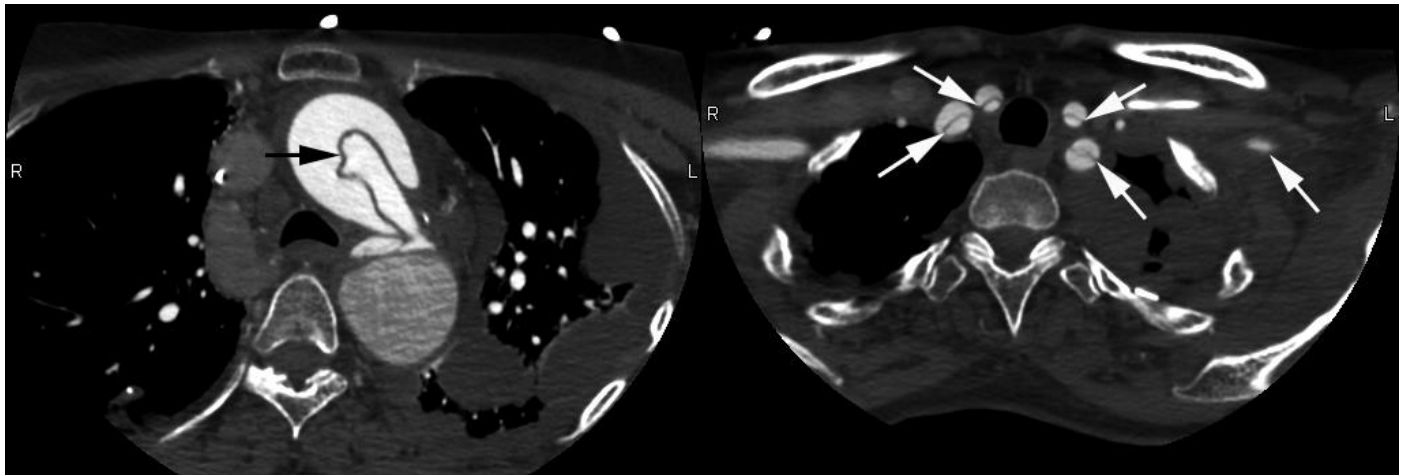
Figure 1: 51-year-old female with Marfan syndrome and blindness secondary to bilateral retinal detachment.
FINDINGS: A. Axial contrast enhanced CT through the chest in the arterial phase demonstrates Type A dissection involving the aortic arch (black arrow). B. Type A dissection extending into the bilateral common carotid and subclavian arteries (white arrows).
TECHNIQUE: GE (GE lightspeed VCT) 64 slice multidetector CT 646 mAs, 120 kV, 1.3 mm slice thickness.
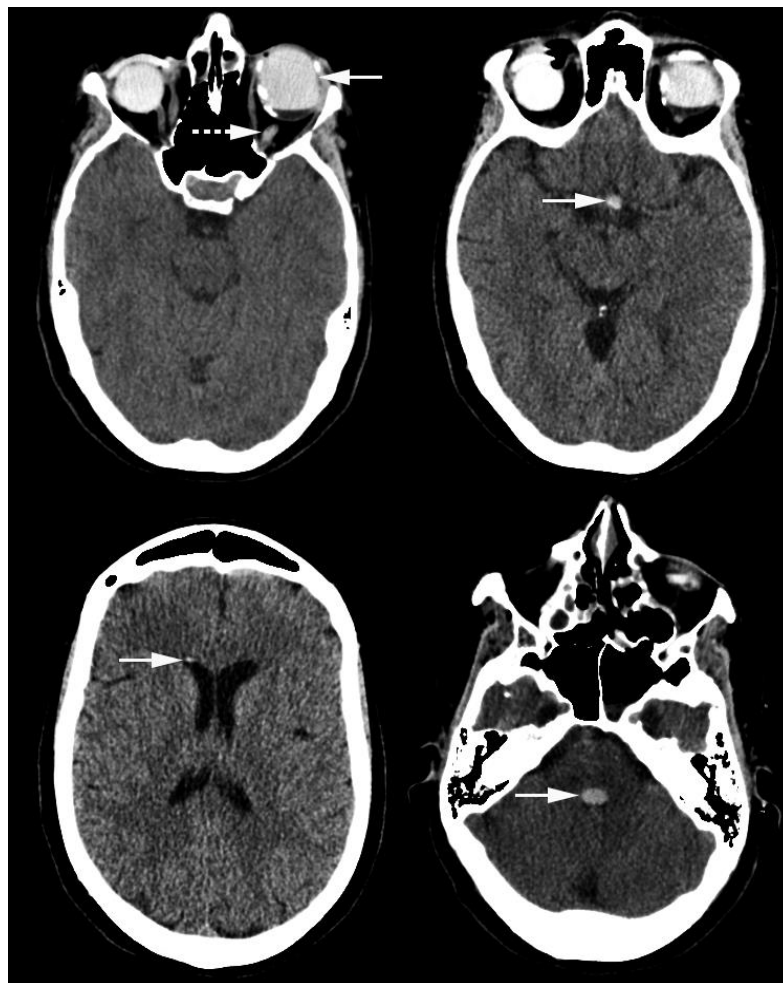
Figure 2: 51-year-old Female with Marfan syndrome and blindness secondary to bilateral retinal detachment.
FINDINGS: Axial CT slices through the brain showing hyperdense silicone mimicking intraventricular hemorrhage in A. The left globe (arrow) tracking in the left optic nerve sheath (dotted arrow), which was not observed on the initial outside report. B. The optic chiasm (white arrow). C. The frontal horn of the right lateral ventricle; the non-dependent nature was not observed on the initial outside report (white arrow). D. The fourth ventricle. HU = 100 (white arrow).
TECHNIQUE: Toshiba CT scanner 250 mAs, 120 kV, 3mm slice thickness.

Figure 3: 51-year-old Female with Marfan syndrome and blindness secondary to bilateral retinal detachment.

FINDINGS: A. Axial FLAIR MR image showing chemical shift artifact at the interface between silicone and adjacent brain parenchyma in the fourth ventricle (white arrow). B. Axial FLAIR MR image showing hyperintense silicone mimicking intraventricular hemorrhage filling the fourth ventricle (white arrow). C. Axial susceptibility weighted MR image showing susceptibility artifact caused by silicone mimicking intraventricular hemorrhage in the fourth ventricle (white arrow). D. E. Axial diffusion weighted image (DWI) and Apparent Diffusion Coefficient (ADC) map at the level of the cerebellum showing lack of restricted diffusion in the silicone filling the fourth ventricle (white arrow). F. Non-contrast axial T1 MR image showing T1 hyperintense silicone within the left globe and along the optic nerve (white arrow). G Non-contrast axial T1 image through the lateral ventricles with T1 hyperintense silicone situated non-dependently in the right frontal horn. H. Axial Gradient Recall Echo (GRE) image through the lateral ventricles showing susceptibility artifact corresponding with T1 hyperintense silicone (white arrow). I. Non-contrast sagittal T1 MR image with hyperintense silicone in the optic chiasm, the third ventricle, and the fourth ventricle (white arrows) mimicking intraventricular hemorrhage.

TECHNIQUE: 1.5T GE MR Scanner (GE discovery 450) Axial T2-FLAIR: 5 mm slice thickness, TR = 8000 ms, TE = 124.3 ms, Flip Angle 160. Axial SWI 2.2 mm slice thickness, TR = 5500 ms, TE = 25 ms, Flip Angle 90. Axial Diffusion Weighted Image 5 mm slice thickness, TR = 8000, TE = 83.7, Flip Angle 90. Axial Apparent Diffusion Coefficient Map: 5 mm slice thickness, TR = 8000, TE = 83.7, Flip Angle 90. Axial T1: 5 mm slice thickness, TR = 500 ms, TE = 12 ms, Flip Angle 90. Axial Gradient Recall Echo: 5 mm slice thickness, TR = 575 ms, TE = 15 ms, Flip Angle 20. Sagittal T1: 5 mm slice thickness, TR = 466.668 ms, TE = 12 ms, Flip Angle 90.
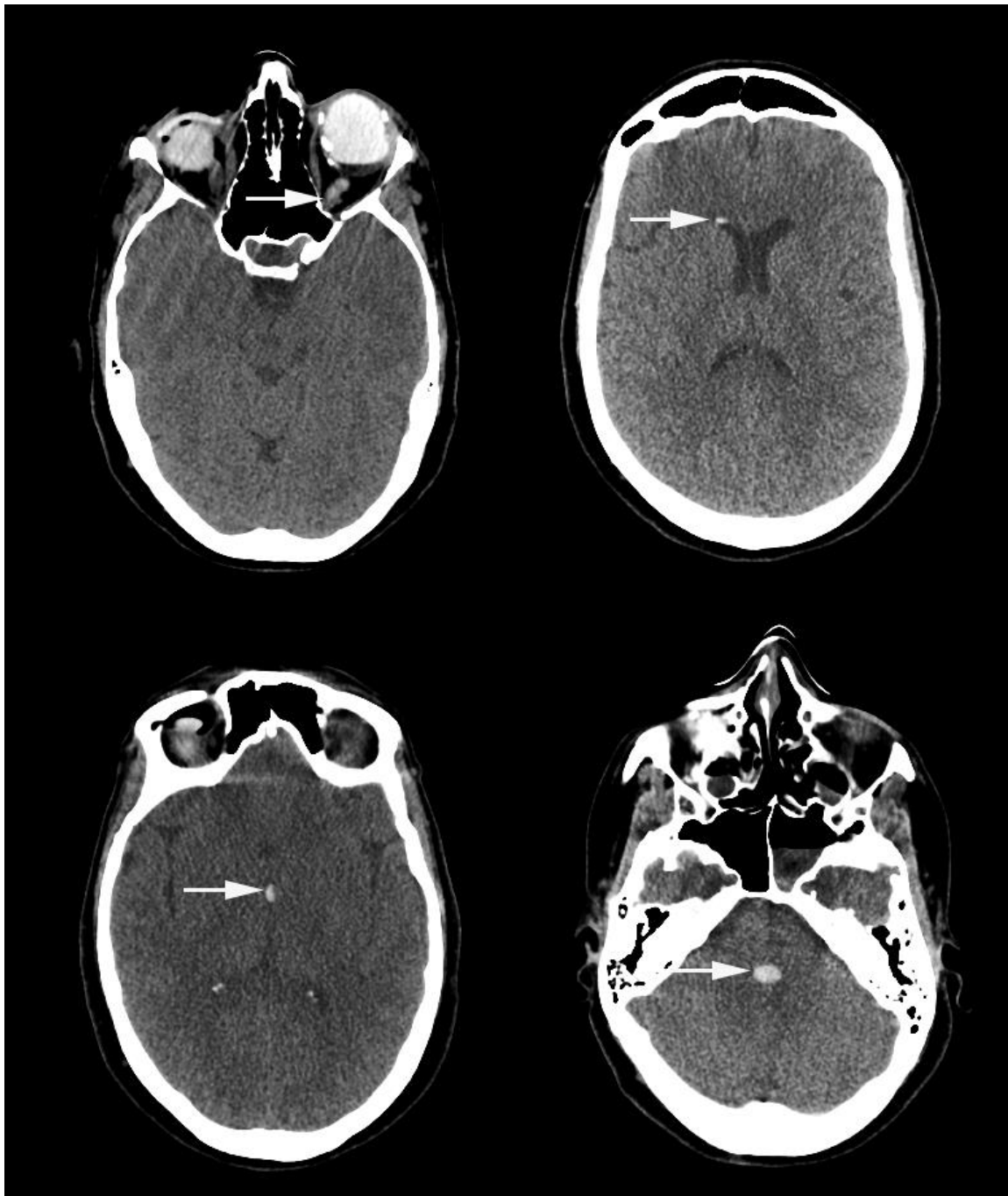
Figure 4: 51-year-old Female with Marfan syndrome and blindness secondary to bilateral retinal detachment.
FINDINGS: Axial CT images taken 4 days after the initial outside CT scan showing A. Hyperdense silicone in the left globe tracking along the left optic sheath (white arrow). B. Hyperdense silicone layering non-dependently in the frontal horn of the right lateral ventricle (white arrow). C. Hyperdense silicone in the third ventricle, identical in position compared with the CT performed 4 days prior (white arrow). D. Hyperdense silicone in the fourth ventricle, also identical in position compared with the prior CT (white arrow). Silicone in the discussed locations was mistaken for hemorrhage.
TECHNIQUE: GE (GE lightspeed VCT) 64 slice multidetector CT 226 mAs, 100 kV, 2.5 mm slice thickness.

Etiology	Intracranial migration of intraocular silicone
Incidence	Uncommon, 14 case reports, 5 in the radiology literature, 20 total patients
Gender Ratio	Unknown, 13 male, 7 female reported patients
Age Predilection	Age range 15 – 80 among reviewed case reports
Postulated Risk Factors	High intraocular pressure, congenital abnormality of the optic nerve such as optic pit, deep cupping of the optic nerve, Marfan syndrome.
Clinical Presentation and Treatment	Often asymptomatic although reported symptoms include headache, nausea, dizziness, seizures, a single case of elevated intracranial pressure treated successfully with ventriculoperitoneal shunt [10]
Prognosis	Unknown, generally an incidental finding
Findings on Imaging	CT: hyperdense HU > 90 MRI: T1 hyperintense to normal vitreous with prominent chemical shift artifact, T2 variable intensity depending on viscosity and pulse sequence parameters, GRE/SWI increased susceptibility artifact, DWI lack of restricted diffusion.

Table 1: Summary table for intracranial migration of intraocular silicone

Entity	CT Findings	MRI Findings
Intracranial Silicone	Hyperdensity in subarachnoid space, non-dependent location in the ventricles with HU > 90.	T1 hyperintense to normal vitreous with chemical shift artifact, T2 variable intensity depending on viscosity and pulse sequence parameters, GRE/SWI increased susceptibility artifact, DWI lack of restricted diffusion. Non-dependent location in the ventricles.
Subarachnoid Hemorrhage	Hyperdensity in subarachnoid spaces with HU 30-60. Dependent location in the ventricles.	T1 isointense to hyperintense at less than 2-3 weeks old, T2 variable intensity, GRE/SWI positive susceptibility artifact/dark, DWI variable restricted diffusion, no chemical shift artifact. Dependent location in the ventricles.
Spontaneous intracranial hypotension	Most commonly normal. May see hyperdensity within the basilar cisterns and Sylvian fissures.	Diffuse pachymeningeal enhancement, sagging brainstem, T2/FLAIR hyperintense dura.
Leptomeningitis	Hyperdensity within the basilar cisterns and Sylvian fissures.	Leptomeningeal enhancement, FLAIR hyperintense signal in the subarachnoid space.
Hypoxic encephalopathy	Hyperdensity within the basilar cisterns and Sylvian fissures.	Gray matter structures affected: Basal Ganglia, thalami, cortex, cerebellum, and hippocampi. DWI: Bright in the first few hours, T1 normal, T2 hyperintensity from 24 hours to two weeks, FLAIR hyperintensity after several days, T1 hyperintensity after two weeks due to cortical laminar necrosis.

Table 2: Differential diagnosis for intracranial migration of intraocular silicone

IMAGING	SILICONE	BLOOD
CT	Hyperdense HU > 90	Hyperdense HU 30-60
MR T1	Hyperintense to normal vitreous	Isointense to hyperintense at less than 2-3 weeks old
MR T2	Variable depending on viscosity and pulse sequence parameters.	Variable
MR GRE/SWI	Susceptibility artifact/dark	Susceptibility artifact/dark
MR Diffusion Restriction	No	Variable
Chemical Shift Artifact	Yes	No

Table 3: Imaging characteristics of silicone vs. blood

AUTHORS	MECHANISM
Shields et al (1989)	Cavernous degeneration of the optic nerve leads to communication between the optic nerve and the subarachnoid space secondary to increased intraocular pressure.
Eller et al (2000)	Increased intraocular pressure allows silicone to infiltrate the optic nerve tissue, pass through the pia mater into the subarachnoid space, CSF space, and ventricular system.
Papp et al (2004)	Silicone transported into the optic nerve through the pia into subarachnoid space secondary to increased intraocular pressure and active transport by macrophages.
Fangtian et al (2005)	Intraocular silicone migration through deep cupping of the optic nerve directly through the pia mater of the brain into the peri-optic subarachnoid space.
Kuhn et al (2006)	Intraocular silicone migration through an optic pit, a congenital depression in the optic nerve head into the subarachnoid space and eventually the ventricular system.

Table 4: Proposed pathways of intraocular silicone to the subarachnoid space/ventricles [4, 25-28]

ORGAN SYSTEM	IMAGING FINDINGS
Cardiovascular	Arterial aneurysms and dissection, pulmonary arterial dilatation, mitral valve prolapse, annuloaortic ectasia
Ocular	Ectopia lentis, retinal detachment, increased axial length of globe, flattening of cornea
Thoracic	Spontaneous pneumothoraces, bullae, blebs and pneumatoceles
Skeletal	Joint (esp. atlanto-axial) subluxation and dislocation, kyphoscoliosis, vertebral body scalloping, increased interpeduncular distance, Schmorl nodes, patella alta, pes planus, hallux valgus, club foot, arachnodactyly, protrusio acetabuli, pectus excavatum, pectus carinatum
Neurologic	Dural ectasia, lumbosacral meningoceles

Table 5: Potential imaging findings in Marfan syndrome [14]

AGE	CT	MR					
Hyperacute (<24 hours)	Hypodense	T1	T2	GRE	DWI/ADC	Hgb	
		Isointense	Hyperintense	+ rim	↑/↓	OxyHgb	
Acute (1-3 days)	Hyperdense 40-60 HU initially, 60-80 HU over hours	Iso to mildly hypointense	Markedly hypointense	+	↓/↓	DeoxyHgb	
Early Subacute (3-7 days)	Attenuation decrease beginning peripherally	Hyperintense peripherally, isointense center	Decreasing hypointensity	+	↓/↓	MetHgb intracellular	
Late Subacute (7-14 days)	Progressive attenuation decrease	Hyperintense	Hyperintense centrally, hypointense peripherally	+ rim	↑/↓	MetHgb extracellular	
Chronic (>14 days)	Hypodense	Iso to hypointense	Hypointense	+	N/A	Hemosiderin	

Table 6: CT and MR characteristics of blood over time [19, 20]

ABBREVIATIONS

CSF = Cerebrospinal fluid
CT = Computed Tomography
CTA = CT angiography
FLAIR = Fluid attenuated inversion recovery
GRE = Gradient Recall Echo
HU = Hounsfield Units
ICU = Intensive care unit
MRI = Magnetic resonance imaging
OR = Operating room
SAH = Subarachnoid hemorrhage
SIH = Spontaneous intracranial hypotension
SWI = Susceptibility Weighted Image
T1WI = T1-weighted imaging
T2WI = T2-weighted imaging

KEYWORDS

Intraocular silicone; intracranial silicone; retinal detachment; Marfan syndrome; intraventricular hemorrhage; intracranial hemorrhage

www.RadiologyCases.com